In vitro RABiT measurement of dose rate effects on radiation induction of micronuclei in human peripheral blood lymphocytes

Antonella Bertucci, **Lubomir B. Smilenov**, **Helen C. Turner**, **Sally A. Amundson**, and **David J. Brenner**

Center for Radiological Research Columbia University Medical Center 630 W. 168th St. New York, NY 10032

Abstract

Developing new methods for radiation biodosimetry has been identified as a high priority need in case of a radiological accident or nuclear terrorist attacks. A large-scale radiological incident would result in an immediate critical need to assess the radiation doses received by thousands of individuals. Casualties will be exposed to different doses and dose-rates due to their geographical position and sheltering conditions, and dose-rate is one of the principal factors that determine the biological consequences of a given absorbed dose. In these scenarios high-throughput platforms are required to identify the biological dose in a large number of exposed individuals for clinical monitoring and medical treatment. The RABiT (Rapid Automated Biodosimetry Tool) is designed to be completely automated from the input of blood sample into the machine to the output of a dose estimate. The primary goal of this paper was to quantify the dose-rate effects for RABiT-measured micronuclei *in vitro* in human lymphocytes. Blood samples from healthy volunteers were exposed *in vitro* to different doses of X-rays to acute and protracted doses over a period up to 24 hours. The acute dose (ADR) was delivered at ∼1.03Gy/min and the low dose rate (LDR) exposure at ∼0.31Gy/min. The results showed that the yield of micronuclei decreases with decreasing dose-rate starting at 2Gy, whereas response was indistinguishable from that of acute exposure in the low dose region, up to 0.5Gy. The results showed a linear-quadratic dose-response relationship for the occurrence of micronuclei for the acute exposure and a linear dose-response relationship for the low dose-rate exposure.

Introduction

The development of improved methods for radiation biodosimetry has been identified as a high priority need in an environment of heightened concern over possible radiological or nuclear terrorist attacks [1, 2]. The detonation of even a small Radioactive Dispersal Device (RDD) in a large metropolitan area would be likely to create large-scale panic, despite the low risk of radiological injuries. A small Improvised Nuclear Device (IND) would produce a major health emergency in addition to mass panic. In such situations, in that the general population would not be carrying physical dosimeters, a very high throughput means of assessing the radiation exposure based on biological endpoints will be needed. This will serve both to reduce panic by reassuring those who were not significantly exposed, as well as triaging those in need of medical attention [3].

When planning for the response to an IND detonation, it is assumed that radiation exposure will occur through two pathways: prompt radiation near the site of the detonation, which gives off radiation at a high dose rate, and residual radiation (fallout), which has a lower dose rate. Therefore, these scenarios involve significant components of the dose being delivered over many hours. Also, the total absorbed dose is dependent on location and duration of exposure. Sheltering on-site during the initial phase (hours to one day) can considerably reduce exposure [4]. There will be the "Dangerous Fallout Zone" (DFZ) in which victims will be at risk for acute radiation syndrome (ARS), and this zone will reach its maximum extent after the first few hours and then shrink in size in just one day [5].

Computer models indicate that within about 24 hours of a 10 KT IND detonation, the most significant fallout hazard area will extend 10 to 20 miles from ground zero. Within a few miles of ground zero, exposure rates in excess of 100 R/h during the first four to six hours post-detonation may be observed. 24 hours post-detonation the estimated dose-rate in the same conditions will reach a value of $\sim$0.38cGy/min. The NCRP recommend defining the perimeter of the DFZ as an area with an exposure rate of 10 R/h ($\sim$0.1 Gy h-1 air-kerma rate). In a DFZ external exposure to gamma radiation is the dominant health concern; however, β radiation can cause severe tissue damage when fallout material remains in contact with unprotected skin.

Casualties inside the DF zone will be exposed to different dose-rates due to their geographical position and sheltering conditions. Dose rate is one of the principal factors that determine the biological consequences of a given absorbed dose [6-8]. As the dose rate is lowered and the exposure time extended, the biologic effect of a given dose generally is reduced [4]. It is well known that the dose rate effect must be considered when evaluating risks since many studies reported a significant biological reduced response with decrease of the dose rate [5].

Among the casualties of an IND thousands of persons would be exposed to radioactive fallout downwind from the explosion. Such victims might be exposed to substantial doses of radiation, but without clear signs and symptoms of radiation toxicity or exposure initially. There is thus a need for rapid, accurate and sensitive diagnostic platforms that can confirm exposure and estimate the radiation dose absorbed [9].

In large-scale events such as an IND, rapid tools are required to identify the physical dose individuals were exposed to in order to provide appropriate clinical monitoring and treatment [10]. The principle of biodosimetry is to utilize changes induced in the individuals by ionizing radiation to estimate the dose and, if possible, to predict or reflect the clinically relevant dose. Emerging biodosimetric techniques utilize changes in tissues of individuals exposed to ionizing radiation as a quantitative measure of the absorbed dose[11]. Several recent approaches for biodosimetry include biological response to ionizing radiation through gene expression [12] protein products [13] or measures of products of altered metabolism [14-17]. However, more mature assays, such as the dicentric chromosome assay (DCA) and the cytokinesis-block micronucleus assay (CBMN) in peripheral blood lymphocytes (PBL) have been extensively validated as biodosimeters for dose estimation purposes [18-24].

Compared to the DCA, considered the "gold standard" for biological dosimetry, the CBMN is characterized by very easy and rapid scoring. This feature in addition to its good reliability and reproducibility [25] makes this method very attractive for large scale assessment of genetic damage in radiation workers [19] and for population triage in case of a large scale radiation accident [26]. Several reports have demonstrated that the CBMN assay can detect dose rate effects in micronuclei (MNi) yields, namely a decrease with decreasing dose rate, reflecting increased repair [27-29].

Following a large scale radiological event, the first responders will be able to reach the location of the accident in a few hours after the initial event [30]. It is estimated that the earliest organized emergency response will be capable of collecting samples for an initial victim triage of the accident in not less than 24 hours post-event [5, 30]. These collection sites will require advanced high-throughput biodosimetry platforms [4]. Over the past years our group has developed such a platform, the RABiT (Rapid Automated Biodosimetry Tool). The RABiT completely automates three well-established biodosimetry assays, the CBMN [31, 32], the yield of phosphorylation of the histone H2AX (γ-H2AX assay) [33-35] and the dicentric assay [36]. The RABiT allows high throughput analysis of thousands of blood samples per day, providing a dose estimate of past radiation exposure that can be used to support clinical triage and treatment decisions [37].

The primary goal of this paper was to quantify the dose-rate effects for RABIT-measured micronuclei *in vitro* in human lymphocytes. For the MNi assay, studies aimed at characterizing the dose-rate effect for radiation induced micronuclei in human lymphocytes showed that the MNi yield decreases with decreasing dose rate [27, 29, 38, 39]. Furthermore, it has been demonstrated that the MNi response curve in human peripheral lymphocytes decreased with decreasing dose rate, becoming more curvilinear, with a pure linear response of MNi induction observed at lowest dose rate [27]. However, all these studies were performed with the standard CBMN, in which blood samples exposed to ionizing radiation are processed immediately or in a short period of time (from minutes to a few hours) after irradiation.

In addition to our primary goal, we measure in a realistic scenario, how the RABiT-measured micronuclei yield in human lymphocytes changes with exposure time, over periods of up to 24 hours, compared to acute (few seconds) exposure. Furthermore, in order to validate the RABiT-measured micronuclei frequencies 24 hours post irradiation, we compared the results obtained with micronuclei frequencies measured in blood samples exposed with the same ADR modalities and doses and processed in the standard CBMN assay (within 1 hour post irradiation).

Materials and Methods

Experimental Design

Our main assumption is that following a large scale radiological event the first responders will be able to reach the location of the accident after 24 hours post irradiation. Therefore, the experimental design selected for this study considers that blood samples will be obtained 24 hrs post-detonation from victims who have been exposed to a variety of dose-rates and

doses. Those individuals who were close to the explosion area would be exposed to high doses of radiation at a high dose rate (ADR). Conversely, people who were located a certain distance from the source of radiation or who were shielded (e.g. those inside buildings) would be exposed with a low dose rate modality (LDR).

Human blood was exposed *in vitro* to different acute and protracted doses of X-rays over a period of 24 hours. The acute dose rate (ADR) exposure was delivered at ~1.03 Gy/min and the low dose rate (LDR) exposure at ~0.31 cGy/min. Assuming that in a realistic scenario the earliest samples could be collected would be 24 hours post irradiation, MNi frequencies were measured *in vitro* using the cytokinesis blocked micronucleus assay in peripheral lymphocytes 24 hours post irradiation.

In addition, another set of blood samples were irradiated with the same modalities of the ADR exposure and cultured immediately after exposure (T=0) to validate the RABiT-measured MNi 24 hours post exposure compared to the standard *in vitro* CBMN assay [31], in which samples are cultured from minutes to one hour post irradiation.

Donors

Whole blood was collected from twelve healthy volunteers (6 males and 6 females) at Columbia University Medical Center. The age range was between 26 and 46 years old. Informed consent was obtained from all volunteers according to IRB protocol. The donors were required to fill in an anonymous questionnaire to ensure that they had not been exposed to ionizing radiation in the previous two years before the blood draw in order to minimize the effect of ionizing radiation as a confounding factor. For each donor, 12mL of blood was drawn by venipuncture into spray coated sodium heparin (158 USP) vacutainer tubes (Becton Dickinson and Company, Franklin Lakes, NJ). Blood samples were aliquoted into 1 mL samples and transferred to a centrifuge tube (50mL volume); to each sample was added to 3mL of complete culture medium (RPMI 1640 +10% FBS 1% Pen/Strep; Invitrogen, Carlsbad, CA) without phytoemagglutinin (PHA). The contents were mixed gently and the tubes were positioned in the irradiation chamber for radiation exposure.

Irradiation Source and dosimetry

Sample irradiations were performed using the X-Rad 320 Irradiator (Precision X-Ray, North Branford, CT). For our studies, dose and dose rate were achieved by using a custom made Thoraeus filter (1.25 mm Sn, 0.25 mm Cu, 1.5 mm Al). The filter provided a dose rate of 0.31cGy/min (4.4Gy for 24 hours) at the maximum source to surface distance (SSD), 50 cm, for the low-dose rate regime and 1.03 Gy/min at 40 cm SSD for the acute dose rate regime.

The X-Rad machine was calibrated using an N30013 ion chamber (PTW Farmer, Freiburg, Germany). During the actual irradiations, the delivery dose and the dose rate were monitored and measured in real time by a dose measuring parallel plate transmission chamber located inside in the filter holder assembly of the X-Rad machine. Doses of 0.56, 2.23 and 4.45Gy were used for the acute and low dose irradiations.

Low dose rate experiments required the maintenance and exposure of blood samples for several hours under constantly controlled environmental conditions (37°C, 5% CO_2 and

80% humidity). To fulfill this requirement we built a custom incubator mainly made of plastic to avoid scattering radiation. Temperature was controlled through solid state heaters on a feedback loop attached to the walls of the incubator to distribute the heat evenly. This setting maintained a temperature of 37°C ($\pm$ 0.5°C). The CO_2 concentration, humidity and temperature within the incubator were monitored using data loggers. Blood was exposed in 50mL conical tubes angled to keep the samples within about a 20cm diameter in order to minimize planar dose variation. The tube holder was rotated at speed of 3 rotations per hour to further minimize any dose inhomogeneity.

The ADR samples after irradiation were transferred to a CO_2 incubator and incubated for 24 hours before processing.

Micronucleus assay

Irradiated blood sample were gently mixed and for each sample 2mL of blood mixed with medium was transferred to culture flask and supplemented with extra fresh medium containing 2% PHA for initiation of the culture. Cells were incubated for 44 hours (37°C, 5% CO_2, 98% humidity); following incubation, cytochalasin-B (Sigma Aldrich, St. Louis, MO) at a final concentration of 6μg/mL was added to block the cytokinesis after PHA stimulation.

Cells were harvested at 70 hours. The contents of the flasks were transferred to a 15mL centrifuge tube and the tubes were centrifuged for 10min at 1000 RPM to pellet the lymphocytes. Cells were treated with 0.075M HCl solution at room temperature for 10 minutes and then fixed with ice cold fixative (methanol/ acetic acid 3:1).

The fixed cells were then stored in a fire-proof fridge overnight and then moved to a -20°C fire-proof freezer. Prior to slide preparation the lymphocytes were centrifuged and the supernatant discarded. The pellet was re-suspended with fresh fixative solution and the lymphocyte suspension was dropped at the center of a microscope slide and spread by tilting the slide. The slides were allowed to air dry for 10 min before staining through the application of 50μL of DAPI Vectashield mounting medium (Vector Labs, Burlingame, CA) and a cover slip. Slides were left overnight in the fridge prior to imaging.

Imaging and image analysis

Slides were imaged on a Zeiss epifluorescent microscope (Axioplan2 imaging MOT, Carl Zeiss, Germany) driven by MetaferMNScore software (MetaSystems, Althaussen, Germany). The MetaferMNScore automatically scans slides prepared for the cytokinesis-block micronucleus assay. Micronuclei in bi-nucleate cells were visually scored by the inspection of the cell gallery generated by the software. Each data point shown in Fig.1 and Fig. 2 correspond to the average of micronuclei frequencies obtained from 12 samples analyzed individually. For each sample $\sim$ 1000 binucleate cells were scored. Table 1 and table 2 show the micronuclei frequencies, the average and the SEM for each data point.

Statistics

Data obtained from the dose response curve after ADR and LDR exposure for MNI scoring is presented as mean ± standard error of the mean (SEM).

Data for the ADR exposure of lymphocytes cultured at T=0 and T=24 hours after exposure are presented as mean (±SEM) and compared by the 2-tailed Student's t-test indicating statistically no significant differences. The obtained dose response curves were created and fitted using Excel (Microsoft Corp., Redmond, WA).

Results

Micronuclei frequencies were measured using the *in vitro* cytokinesis-blocked micronucleus assay and the data are presented as micronuclei per binucleate cell (MNi/BN). Tables 1 and 2 show the average MNi frequencies measured and the SEM calculated for each data point.

Figure 1 shows the micronuclei frequencies in CBMN lymphocytes cultures after ADR and LDR irradiation.

The results show clearly that the yield of micronuclei decreases with decreasing dose-rate starting at 2Gy, whereas the response was indistinguishable from that to acute exposure in the low dose region, up to 0.5Gy. We found a linear-quadratic dose-response relationship for the occurrence of micronuclei for the acute exposure and a linear dose-response relationship for the low dose-rate exposure.

Figure 2 shows the micronuclei frequencies measured in human lymphocytes after ADR exposure when the cells were cultured immediately after exposure (T=0) and 24 hours post irradiation (T=24). The results show that for all the doses used no statistically significant differences in micronuclei frequencies were detected in the culture conditions used after comparison with the 2-tailed Student's t-test (p-values< 0.01).

Discussion

The main thrust of this paper is the characterization of a high throughput biodosimetry platform (RABiT) for dose reconstruction and risk assessment under mass-casualty scenarios such as an IND. In the present study, we analyzed the RABiT-measured *in vitro* dose response relationship for micronuclei induction in human lymphocytes after acute and protracted x-ray irradiation. The scenario considered in this study is modeled after a IND event were it is estimated that the earliest organized emergency response will be capable of collecting samples at the earliest 24 hours post-event from casualties inside the DFZ. Victims in these areas will be exposed to different dose-rates due to their geographical position and sheltering conditions. Therefore, it is critical to characterize dose rate effects on the yield of MNi as well as the timing of sampling for the use of the RABiT system under a realistic concept of operations.

The results obtained showed that the micronuclei yield increases monotonically with the dose. While in the low dose region the yield of micronuclei remain essentially the same for both ADR and LDR, the results show clearly that for radiation doses higher than 2Gy the

yield of micronuclei decreases with decreasing dose-rate. The ADR response has a linear quadratic trend where the LDR response increases linearly with the dose.

To further characterize the RABiT-measured frequencies of micronuclei, the results obtained for the ADR 24 hours post irradiation were compared with the frequencies measured in samples cultured in the standard CBMN assay modality (samples processed within an hour post irradiation: T=0) using the same irradiation doses and set up. Two-tailed t-test analysis showed that there were no statistically significant differences in the dose response for each dose analyzed for both processing conditions. These results confirm the usefulness of the RABiT-measured micronuclei yield for dose reconstruction purposes as well as for DNA damage evaluation. The CBMN assay in peripheral blood lymphocytes is a well-established biological dosimetry tool for evaluation of radiation exposure and/or to evaluate the extent of DNA damage, for instance after an environmental, occupational or medical exposure. Because of its good reliability and reproducibility the CBMN has become one of the standard cytogenetic techniques for genetic toxicology and in the field of radiation protection. The micronucleus assay has been thoroughly validated as a radiation biomarker *in vivo* in radiotherapy patients treated with large-field radiation as well in large scale monitoring of nuclear power plant workers and hospital workers [26]. An important advantage of the micronucleus assay is that the signal is stable for months after exposure, with a biological half-life of about 12 months, so the need for early acquisition of blood samples is removed [19].

A large-scale radiological incident would result in an immediate critical need to assess the radiation doses received by thousands of individuals to allow for prompt triage and appropriate medical treatment. These persons might be exposed to substantial doses of ionizing radiations but may not show, at least initially, clear signs and symptoms of radio toxicity. Rapid assessment tools for immediate determination of absorbed dose will then be extremely helpful for screening and triage in case of a mass casualty incident.

The authors believe that automating well-established bioassays represents a valid approach to high-throughput radiation biodosimetry both because a high throughput is achieved but also because, as we have demonstrated here, the RABiT can assess absorbed dose. These characteristics in addition to collection of data about geographical position and sheltering conditions of exposed individuals will allow the rapid screening/triage of people exposed to a variety of doses and dose-rates.

This capability can be enhanced by the addition of exposed individual data about geographical location and sheltering condition allowing the rapid screening/triage of victims exposed to a variety of doses and dose-rates.

References

1. Pellmar TC, Rockwell S. G. Radiological/Nuclear Threat Countermeasures Working. Priority list of research areas for radiological nuclear threat countermeasures. Radiat Res. 2005; 163(1):115–23. [PubMed: 15606315]

2. Kulka U, et al. Realising the European network of biodosimetry: RENEB-status quo. Radiat Prot Dosimetry. 2015; 164(1-2):42–5. [PubMed: 25205835]

3. Garty G, et al. The RABIT: a rapid automated biosimetry tool for radiological triage. Health Phys. 2010; 98(2):209–17. [PubMed: 20065685]

4. Knebel AR, et al. Allocation of scarce resources after a nuclear detonation: setting the context. Disaster Med Public Health Prep. 2011; 5(Suppl 1):S20–31. [PubMed: 21402809]

5. DiCarlo AL, et al. Radiation injury after a nuclear detonation: medical consequences and the need for scarce resources allocation. Disaster Med Public Health Prep. 2011; 5(Suppl 1):S32–44. [PubMed: 21402810]

6. Hall EJ. Weiss lecture. The dose-rate factor in radiation biology. Int J Radiat Biol. 1991; 59(3):595–610. [PubMed: 1672350]

7. Vilenchik MM, Knudson AG. Radiation dose-rate effects, endogenous DNA damage, and signaling resonance. Proc Natl Acad Sci U S A. 2006; 103(47):17874–9. [PubMed: 17093045]

8. Turesson I. Radiobiological aspects of continuous low dose-rate irradiation and fractionated high dose-rate irradiation. Radiother Oncol. 1990; 19(1):1–15. [PubMed: 2236638]

9. Ramakrishnana N, Brenner D. Predicting Individual Radiation Sensitivity: Current and Evolving Technologies. Radiation Research. 2008; 170(5):666–675.

10. Jaworska A, et al. Operational guidance for radiation emergency response organisations in Europe for using biosimetric tools developed in EU MULTIBIODOSE project. Radiat Prot Dosimetry. 2015; 164(1-2):165–9. [PubMed: 25274532]

11. Swartz HM, et al. Comparison of the Needs for Biosimetry for Large-scale Radiation Events for Military versus Civilian Populations. Health Phys. 2014; 106(6):755–63. [PubMed: 24776910]

12. Paul S, Amundson SA. Development of gene expression signatures for practical radiation biosimetry. Int J Radiat Oncol Biol Phys. 2008; 71(4):1236–1244. [PubMed: 18572087]

13. Marchetti F, et al. Candidate protein biosimeters of human exposure to ionizing radiation. Int J Radiat Biol. 2006; 82(9):605–39. [PubMed: 17050475]

14. Laiakis EC, et al. Metabolic phenotyping reveals a lipid mediator response to ionizing radiation. J Proteome Res. 2014; 13(9):4143–54. [PubMed: 25126707]

15. Goudarzi M, et al. The effect of low dose rate on metabolomic response to radiation in mice. Radiat Environ Biophys. 2014; 53(4):645–57. [PubMed: 25047638]

16. Goudarzi M, et al. Development of urinary biomarkers for internal exposure by cesium-137 using a metabolomics approach in mice. Radiat Res. 2014; 181(1):54–64. [PubMed: 24377719]

17. Coy SL, et al. Radiation metabolomics and its potential in biosimetry. Int J Radiat Biol. 2011; 87(8):802–23. [PubMed: 21692691]

18. Padovani L, et al. Cytogenetic study in lymphocytes from children exposed to ionizing radiation after the Chernobyl accident. Mutat Res. 1993; 319(1):55–60. [PubMed: 7690459]

19. Thierens H, et al. Cytogenetic biosimetry of an accidental exposure of a radiological worker using multiple assays. Radiat Prot Dosimetry. 2005; 113(4):408–14. [PubMed: 15797919]

20. Voisin P, et al. The cytogenetic dosimetry of recent accidental overexposure. Cell Mol Biol (Noisy-le-grand). 2001; 47(3):557–64. [PubMed: 11441964]

21. Voisin P, et al. Criticality accident dosimetry by chromosomal analysis. Radiat Prot Dosimetry. 2004; 110(1-4):443–7. [PubMed: 15353688]

22. Fenech M. The lymphocyte cytokinesis-block micronucleus cytome assay and its application in radiation biosimetry. Health Phys. 2010; 98(2):234–43. [PubMed: 20065688]

23. Thierens H, et al. Is a semi-automated approach indicated in the application of the automated micronucleus assay for triage purposes? Radiat Prot Dosimetry. 2014; 159(1-4):87–94. [PubMed: 24743767]

24. Rothkamm K, et al. Comparison of established and emerging biosimetry assays. Radiat Res. 2013; 180(2):111–9. [PubMed: 23862692]

25. Fenech M. Cytokinesis-block micronucleus assay evolves into a "cytome" assay of chromosomal instability, mitotic dysfunction and cell death. Mutat Res. 2006; 600(1-2):58–66. [PubMed: 16822529]

26. Thierens H, Vral A. The micronucleus assay in radiation accidents. Ann Ist Super Sanita. 2009; 45(3):260–4. [PubMed: 19861730]

27. Bhat NN, Rao BS. Dose rate effect on micronuclei induction in cytokinesis blocked human peripheral blood lymphocytes. Radiat Prot Dosimetry. 2003; 106(1):45–52. [PubMed: 14653325]

28. Boreham DR, et al. Dose-rate effects for apoptosis and micronucleus formation in gamma-irradiated human lymphocytes. Radiat Res. 2000; 153(5 Pt 1):579–86. [PubMed: 10790279]

29. Sorensen KJ, et al. The in vivo dose rate effect of chronic gamma radiation in mice: translocation and micronucleus analyses. Mutat Res. 2000; 457(1-2):125–36. [PubMed: 11106804]

30. Pellmar TC, Rockwell S. Priority list of research areas for radiological nuclear threat countermeasures. Radiat Res. 2005; 163(1):115–23. [PubMed: 15606315]

31. Fenech M. Cytokinesis-block micronucleus cytome assay. Nat Protoc. 2007; 2(5):1084–104. [PubMed: 17546000]

32. Lyulko OV, et al. Fast image analysis for the micronucleus assay in a fully automated high-throughput biodosimetry system. Radiat Res. 2014; 181(2):146–61. [PubMed: 24502354]

33. Redon CE, et al. γ-H2AX as a biomarker of DNA damage induced by ionizing radiation in human peripheral blood lymphocytes and artificial skin. Advances in Space Research. 2009; 43(8):1171–1178. [PubMed: 20046946]

34. Turner HC, et al. Adapting the gamma-H2AX assay for automated processing in human lymphocytes. 1. Technological aspects. Radiat Res. 2011; 175(3):282–90. [PubMed: 21388271]

35. Garty G, et al. An automated imaging system for radiation biodosimetry. Microscopy Research and Technique. 2015; 78(7):587–598. [PubMed: 25939519]

36. Repin M, et al. Next generation platforms for high-throughput biodosimetry. Radiat Prot Dosimetry. 2014; 159(1-4):105–10. [PubMed: 24837249]

37. Garty G, et al. The RABiT: a rapid automated biodosimetry tool for radiological triage. II. Technological developments. Int J Radiat Biol. 2011; 87(8):776–90. [PubMed: 21557703]

38. Geard CR, Chen CY. Micronuclei and clonogenicity following low- and high-dose-rate gamma irradiation of normal human fibroblasts. Radiat Res. 1990; 124(1 Suppl):S56–61. [PubMed: 2236512]

39. Scott D, Hum Q, Roberts SA. Dose-rate sparing for micronucleus induction in lymphocytes of controls and ataxia-telangiectasia heterozygotes exposed to 60Co gamma-irradiation in vitro. Int J Radiat Biol. 1996; 70(5):521–7. [PubMed: 8947533]
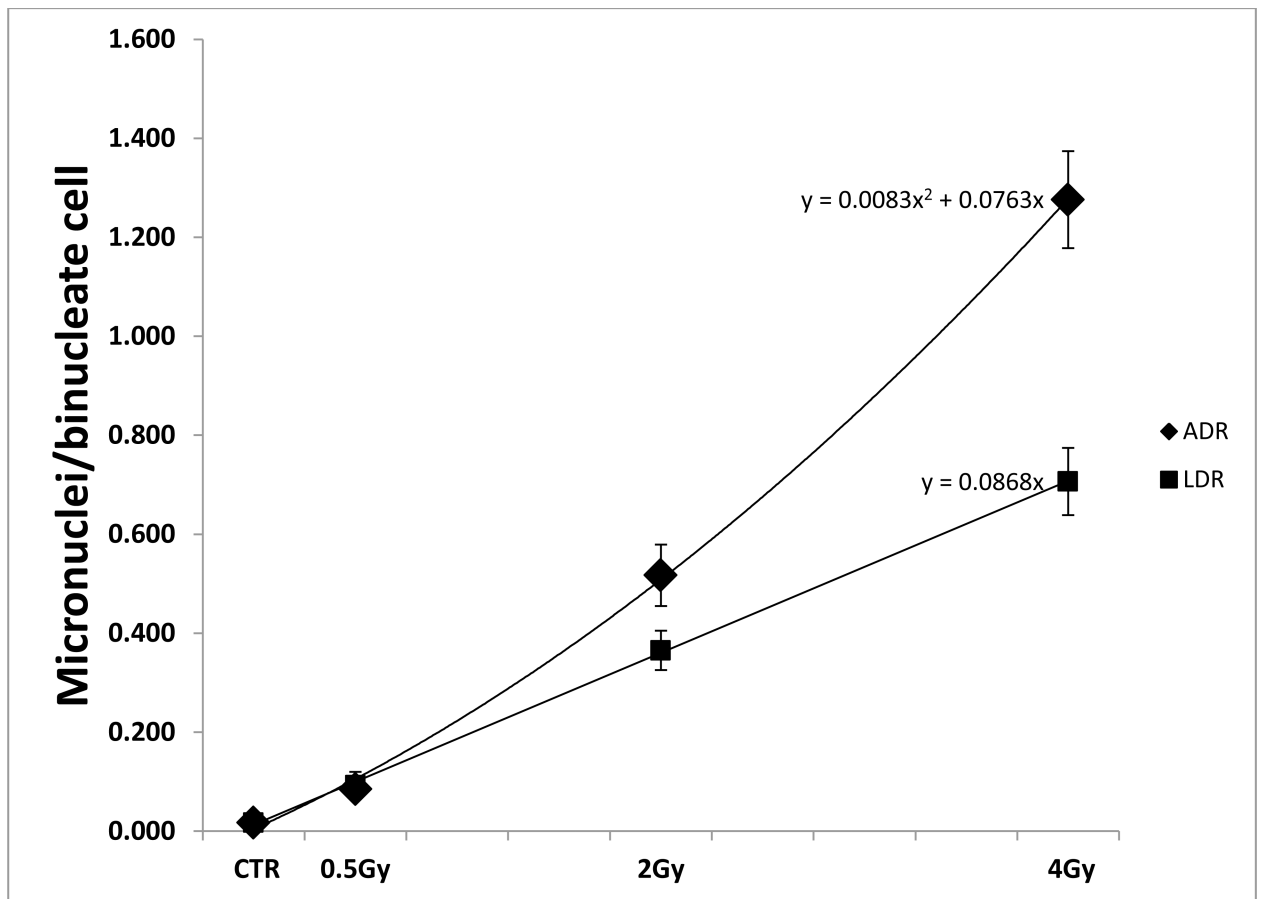
Fig. 1.
The graph shows the RABiT measured dose response curve for micronuclei induction after x-ray irradiation administered with High Dose Rate (ADR) and Low Dose Rate (LDR) modalities. The bars indicate the standard error of the mean.
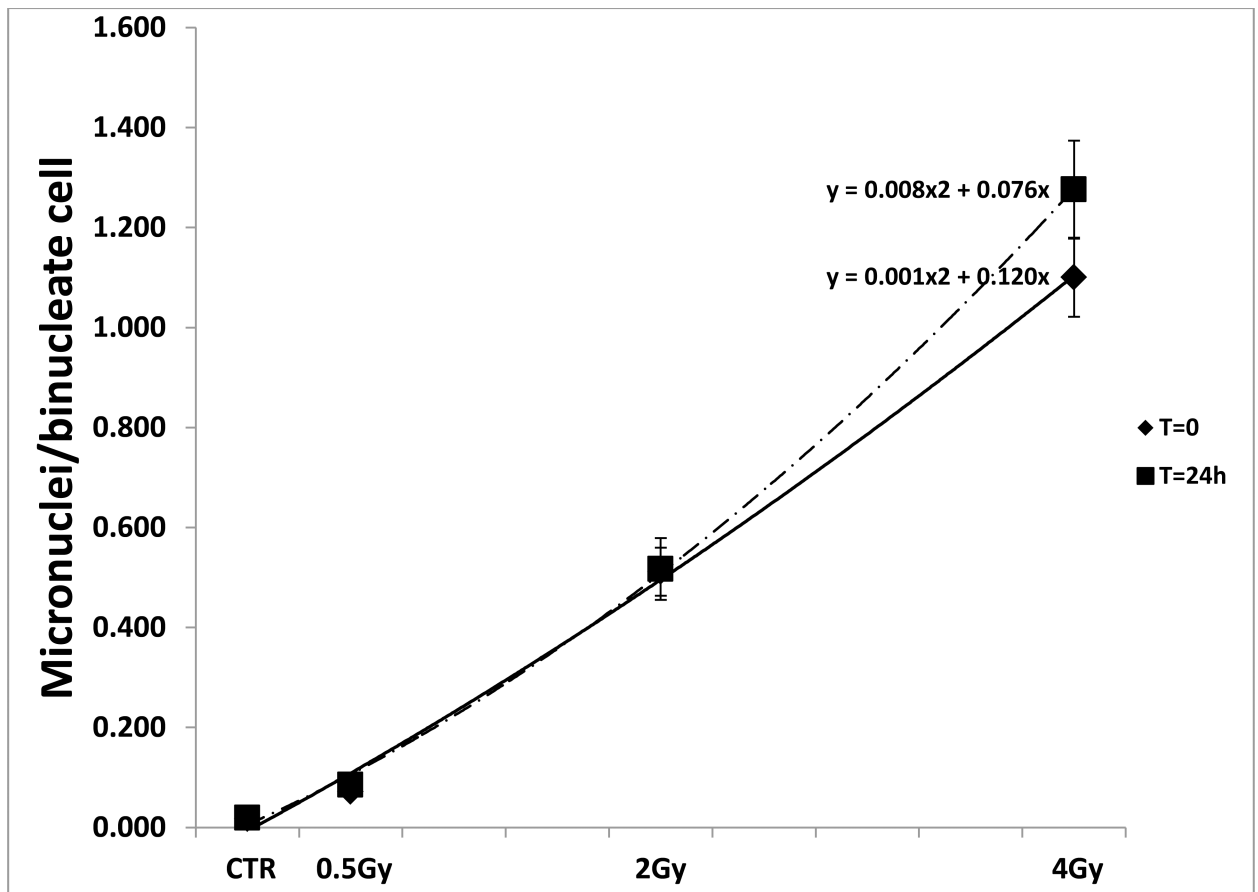
Fig. 2.
The graph shows the RABiT measured dose response curves for micronuclei induction after x-ray irradiation delivered with High Dose Rate (ADR) and processed 24 hours post irradiation (T=24h) and within an hour post irradiation (T=0). The bars indicate the standard error of the mean.

Tab. 1

Micronuclei frequencies measured in samples exposed to graded doses of x-rays in both ADR and LDR scenario. The average frequencies and SEM calculated for each data point is also shown

| Donor | ADR Experiment Dose | | | | | LDR Experiment Dose | | | | |
	0Gy	0.5Gy	2Gy	4Gy	0Gy	0.5Gy	2Gy	4Gy
D1	0.027	0.039	0.116	1.514	0.008	0.054	0.121	0.192
D2	0.008	0.037	0.131	1.010	0.008	0.034	0.167	0.366
D3	0.032	0.115	0.571	1.072	0.036	0.089	0.401	0.812
D4	0.011	0.060	0.507	1.122	0.011	0.389	0.337	0.597
D5	0.029	0.104	0.715	1.491	0.029	0.089	0.388	0.707
D6	0.029	0.074	0.550	1.624	0.010	0.062	0.645	0.784
D7	0.012	0.116	0.62	0.98	0.010	0.066	0.41	0.718
D8	0.015	0.101	0.494	1.139	0.015	0.100	0.318	0.782
D9	0.019	0.097	0.855	1.603	0.019	0.075	0.523	1.077
D10	0.015	0.106	0.489	0.703	0.029	0.094	0.358	0.716
D11	0.011	0.095	0.672	1.875	0.014	0.078	0.351	0.906
D12	0.019	0.080	0.483	1.179	0.018	0.078	0.364	0.822
Average	0.019	0.085	0.517	1.276	0.017	0.101	0.365	0.707
SEM	0.002	0.008	0.062	0.098	0.003	0.027	0.040	0.068

Tab. 2

Micronuclei frequencies measured in samples exposed to graded doses of x-rays and cultured at T=0 and T=24 hours post irradiation. The average frequencies and SEM calculated for each data point is also shown

Donor	T=0 h Experiment Dose				T=24 h Experiment Dose			
	0Gy	0.5Gy	2Gy	4Gy	0Gy	0.5Gy	2Gy	4Gy
D1	0.014	0.030	0.029	1.324	0.027	0.039	0.116	1.514
D2	0.011	0.052	0.490	0.943	0.008	0.037	0.131	1.010
D3	0.034	0.099	0.602	0.896	0.032	0.115	0.571	1.072
D4	0.015	0.061	0.480	0.998	0.011	0.060	0.507	1.122
D5	0.016	0.089	0.550	1.147	0.029	0.104	0.715	1.491
D6	0.018	0.060	0.522	1.500	0.029	0.074	0.550	1.624
D7	0.026	0.083	0.60	0.93	0.012	0.116	0.62	0.978
D8	0.007	0.064	0.530	0.948	0.015	0.101	0.494	1.139
D9	0.011	0.090	0.728	1.494	0.019	0.097	0.855	1.603
D10	0.019	0.088	0.504	0.685	0.015	0.106	0.489	0.703
D11	0.012	0.078	0.597	1.440	0.011	0.095	0.672	1.875
D12	0.012	0.073	0.508	0.897	0.019	0.080	0.483	1.179
Average	0.016	0.072	0.512	1.101	0.019	0.085	0.517	1.276
SEM	0.002	0.006	0.048	0.079	0.002	0.008	0.062	0.098